ACS Infectious Diseases

Perspective

Cite This: ACS Infect. Dis. 2019, 5, 796−808

pubs.acs.org/journal/aidcbc

Quantifying the Interactions between Biomolecules: Guidelines for Assay Design and Data Analysis

Peter J. Tonge*

Center for Advanced Study of Drug Action, Departments of Chemistry and Radiology, Stony Brook University, John S. Toll Drive, Stony Brook, New York 11794-3400, United States

ABSTRACT: The accurate and precise determination of binding interactions plays a central role in fields such as drug discovery where structure−activity relationships guide the selection and optimization of drug leads. Binding is often assessed by monitoring the response caused by varying one of the binding partners in a functional assay or by using methods where the concentrations of free and/or bound ligand can be directly determined. In addition, there are also many approaches where binding leads to a change in the properties of the binding partner(s) that can be directly quantified such as an alteration in mass or in a spectroscopic signal. The analysis of data resulting from these techniques invariably relies on computer software that enable rapid fitting of the data to nonlinear multiparameter equations. The objective of this Perspective is to serve as a reminder of the basic assumptions that are used in deriving these equations and thus that should be considered during assay design and subsequent data analysis. The result is a set of guidelines for authors considering submitting their work to journals such as *ACS Infectious Diseases*.

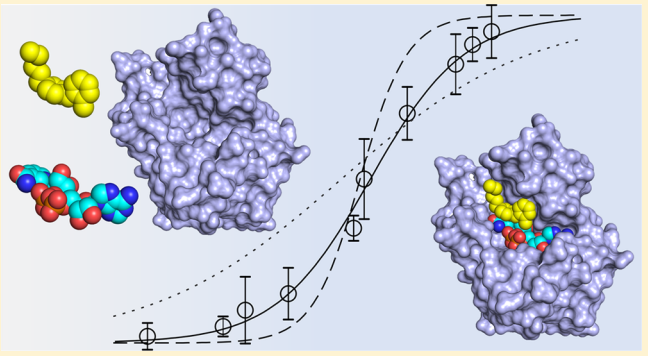

KEYWORDS: *binding, concentration (dose)−response curves, IC_{50}, nonlinear regression, replicates, reproducibility*

Biomolecular interactions, such as protein−protein, protein−ligand, and protein−nucleic acid interactions, occur because the complex that is formed is thermodynamically more stable than the unbound species. However, although thermodynamics provide the driving force for binding, the rate of formation and breakdown of the complex is a function of the transition state barrier on the binding reaction coordinate. A full description of the binding event thus requires parameters such as concentration of inhibitor (ligand) that results in 50% inhibition (effect) (IC_{50}) or K_d values that report on the thermodynamic stability of the complex as well as the on- and off-rates (k_{on} and k_{off}) that quantify the lifetime of the complex. Many methods now exist for determining both the thermodynamics and kinetics of biomolecular interactions and are routinely employed across biological space, for example, by underpinning the generation of structure−reactivity relationships (SARs) or structure−kinetic relationships (SKRs) that guide the selection and optimization of drug leads. This includes competitive radioligand binding,[1] the use of mass spectrometry to quantify unbound ligand,[2] methods that detect binding such as fluorescence (anisotropy, Förster/fluorescence resonance energy transfer (FRET)),[3−6] bioluminescence,[7] or surface plasmon resonance (SPR),[8,9] and assays that monitor change in activity as a function of ligand (agonist, antagonist, inhibitor) concentration.[10]

Access to user-friendly programs that can fit data to nonlinear equations has greatly facilitated the ability of investigators to obtain quantitative insight into their systems. In particular, there is no longer a reliance on linearized transformations of common equations which can distort experimental errors, such as the Scatchard plot for equilibrium binding data and the Lineweaver−Burk plot for enzyme kinetics.[11] However, use of programs such as GraphPad Prism or GraFit to perform nonlinear regression generally requires no knowledge of the assumptions and precepts that underlie the equations used for data analysis. There are of course many excellent, authoritative books and papers on assay design and data analysis. This includes Robert Copeland's book "*Evaluation of enzyme inhibitors in drug discovery: a guide for medicinal chemists and pharmacologists*",[12] and the Assay Guidance Manual (Eli Lilly and NCATS).[13] This Perspective is not intended to replace these sources of information, nor do I attempt to discuss underlying complexities such as the statistics of nonlinear regression.[14] Rather, I seek to raise awareness of some common misunderstandings and thus provide guidelines for authors wishing to publish in ACS ID. In this Perspective, I use the interaction of small molecule chemical compounds with proteins as a paradigm for binding interactions.

RIGOR AND REPRODUCIBILITY: BIOLOGICAL AND TECHNICAL REPLICATES

Many organizations now offer courses and seminars on the Responsible Conduct of Research (RCR). For example, the US National Institutes of Health (NIH) requires that all students funded on NIH grants receive training in RCR.[15] One component of RCR is Data Management, which includes topics such as the

Received: January 14, 2019
Published: March 12, 2019

DOI: 10.1021/acsinfecdis.9b00012
ACS Infect. Dis. 2019, 5, 796−808

rigor and reproducibility of scientific research. Obviously, reproducibility is a fundamental goal in the design and development of appropriate, robust assays for quantifying biomolecular interactions. In this regard, I thought it worth clarifying the difference between biological and technical replicates, which are a component of assessing the reproducibility of scientific findings and often a subject of some misunderstanding. Blainey et al.[16] define biological replicates as "*parallel measurements of biologically distinct samples that capture random biological variation, which may itself be a subject of study or a noise source*", and technical replicates as "*repeated measurements of the same sample that represent independent measures of the random noise associated with protocols or equipment*". Thus, technical replicates provide information on the precision of the measurement method, while biological replicates inform about sample to sample variation in the behavior of separate reagent preps, cell cultures, or animals.[17] The number of replicates and their treatment in subsequent data analysis, for example, whether or not the replicates are averaged, depends on the type of experiment and its purpose. Below, I briefly introduce nonlinear regression and discuss replicates in the context of curve fitting.

GUIDELINES FOR NONLINEAR REGRESSION

Nonlinear regression is a method for fitting an experimental $x-y$ data set, such as a concentration−response relationship, to a mathematical equation. This is achieved by systematically varying the values of the parameters in the equation until the parameter values giving the best agreement between the data and the equation are found. The best fit is defined as the set of parameter values that minimize the squared differences between the measured and calculated y values, summed over all data points (so-called "least-squares" regression). There are several considerations in applying nonlinear regression, including the choice of model (i.e., the fitting equation), whether any parameters should be constrained (such as the Hill coefficient h in an IC_{50} model), the choice of initial values for each parameter, how replicate data points are treated, deciding whether and how to weight the data points, and how to detect and handle outliers (see Box 1). Although this Perspective does not attempt to discuss each of the above topics, it is possible to give some initial guidelines especially on the treatment of replicates.

Investigators may use whatever level of replication they consider appropriate for measurements that are exclusively aimed at helping make decisions on how best to proceed and that are not intended for publication. However, minimal standards of reproducibility must be met for any result to be publishable, and high standards of reproducibility are required for results on which a major conclusion depends. For example, in general, any IC_{50} value reported in a publication should be determined using replicate (typically triplicate) measurements at each inhibitor concentration, and the entire IC_{50} measurement should be repeated at least once (it being acceptable to use the same enzyme and inhibitor preps) to show that it is reproducible. In characterizing the final, optimized inhibitor compound(s), on which the manuscript's claims of important biological activity or other major conclusions are based, higher levels of replication are typically required. These replicates will ideally include using separate preparations of enzyme and inhibitor. This higher level of rigor is required because the reproducibility of the results obtained using these key compounds is central to the validity of the entire publication, and it is therefore essential to show that the results are reproducible and that activity does not vary in unexpected ways from one enzyme prep to another and/or does not result from some contaminant in the inhibitor prep. Regardless of the experimental design, investigators should clearly specify how many and what kind of replicates were performed for each experiment reported (see Box 1).

In an enzymatic assay, the duplicate or triplicate initial velocity measurements at each inhibitor concentration may come from different wells in the same multiwell plate or from individual enzyme assays performed in a cuvette. Assuming that the reagents are stable and the stock solutions are homogeneous (i.e., all components are fully soluble), the differences in the results obtained between the replicate wells provide a measure of the stochastic variability in diluting and dispensing the reagents, plus any irreproducibility in the performance of the detection instrument (e.g., the plate reader). Two different approaches are commonly employed when applying nonlinear regression to such a data set. In one approach, each measurement is treated as an independent data point and the equation is fitted simultaneously to all data points. Alternatively, some investigators will instead average the replicate measurements and then fit the resulting average values to the equation. In most curve fitting programs, it is possible to weight the averaged values according to the spread or the standard deviation of the replicate measurements for each condition. Doing so ensures that the fitting process places greater

Box 1. General Points

(i) Provide full experimental details for each assay including protein and ligand concentrations, buffer conditions, reaction temperature, incubation times, and number of replicates.
(ii) Provide data plots together with the fitted curve(s) and the equation(s) used for the data analysis. Report standard errors for the calculated parameters.
(iii) Nonlinear regression includes the following steps: choice of model, whether to constrain any parameters, selection of initial values for each parameter, whether to use differential weighting, how to detect and handle outliers, and whether to average replicates before data fitting. In general, there should be at least two or better three replicates at each experimental set of conditions (e.g., inhibitor concentration). The replicates can be treated as individual data points in curve fitting, or the averaged data can be analyzed while using the standard deviation of the replicates to weight the data. Fitting averaged data without individually weighting the averaged values should be avoided.
(iv) Parameters for the final, optimized inhibitor compound(s) should ideally be based on replicates determined from separate preparations of enzyme and inhibitor.
(v) Curve fitting programs enable data to be analyzed using very complex mathematical models. Generally, an increase in the number of variables used in data fitting will improve the goodness of fit. However, a valid mechanistic reason must be advanced for increasing the number of variables used to fit the data. This may include information obtained from other approaches. For example, the observation of two different enzyme−inhibitor structures (EI and EI*) by X-ray crystallography supports the two-step slow-onset mechanism for the inhibition of the enoyl-ACP reductase from *Mycobacterium tuberculosis* revealed by progress curve kinetics.[57]

DOI: 10.1021/acsinfecdis.9b00012
ACS Infect. Dis. 2019, 5, 796−808

weight on fitting the averaged values that were determined most precisely, as shown by the close agreement between the replicate measurements, while placing lower weight on fitting values that showed greater differences between the replicates. In general, fitting averaged data without individually weighting the averaged values should be avoided, because it ignores information contained in the data set about the reliability of each measurement. While arguments can be made about the relative statistical validity of averaging or not averaging replicate data points before curve fitting, if the data are of good quality (i.e., reasonably accurate and precise), then the curve fitting will return very similar parameter values regardless of whether the data are averaged and how they are weighted. Conversely, if the data quality is poor, the parameter values resulting from the curve fit will be unreliable, regardless of the fitting approach used.

One lesson arising from the above discussion is that it is important to check the default settings for nonlinear regression used by the curve fitting software to determine how and whether the program weights the different data points in the set. A second point is that, before averaging replicates, it is important to examine the results to check that there is no evidence of systematic error. For example, if data from a plate reader assay shows a significant difference between replicate measurements depending on which row or column of the assay plate the samples occupy, then this is indicative of a systematic rather than a random variation in results. Another common example is the observation that replicate measurements made at various times over the course of a day increase or decrease systematically, indicating that one or more of the reagents is not stable. If systematic error is evident, it is not appropriate to average the measurements. Instead, the source of the systematic error should be identified and eliminated to allow a valid experiment to be performed.

Some common errors in data fitting involve the generation of best-fit parameter values that fall outside scientifically reasonable limits. For example, when fitting a set of inhibitor concentration−response data to an inhibition curve, it is common for investigators who are inexperienced in quantitative analysis to generate curve fits that extrapolate to a reaction velocity below zero at saturating inhibitor concentrations or to a velocity above that of the uninhibited reaction when extrapolated to zero inhibitor. These outcomes are physically impossible, and it is incumbent for the investigators to make sure that the parameter values they obtain after curve fitting their data are indeed reasonable. One approach that can help avoid these errors is to plot the curve fit for a range of x-variable values that extend for at least 2−3 logs above and below the IC_{50}, so that any nonphysical behavior at these extremes of inhibitor concentration becomes apparent. It is often appropriate to constrain the values of one or more parameters in the fitting equation to fix the minimum or maximum y-variable values to known limits or control values. Thus, it is necessary for the investigator to understand the fitting equation (though not necessarily the algorithm by which the data are fit to this equation) and especially that they know which parameter in the equation corresponds to which feature of the fitted curve.

What To Report. Standard errors should be reported for each parameter, and some curve fitting programs will also calculate confidence intervals which could also be reported (see Box 1). If parameters such as IC_{50} values are determined for multiple reagent preps (inhibitor batches/protein preps), then the mean of the values can be reported together with the standard deviation and the number of replicates. In plotting fitted data for publication, the experimental data should be plotted on top of the theoretical curve predicted from the equation using the best-fit parameter values. If the data are averaged, then error bars should be included that represent the range or the standard deviation of the replicate measurements that contributed to each average data point. If the experimental data do not extend to sufficiently low and high values of the x-variable to approach zero effect and a full effect, the line that represents the curve fit should not end at the lowest and highest experimental x-variable values but should extend beyond the data to show that the best-fit equation is consistent with the highest and lowest y-variable values (e.g., full enzyme activity versus zero or background levels of activity) expected from the experiment.

It should be emphasized that these recommendations only scratch the surface of the topic; there is a great deal of additional complexity in curve fitting. For example, curve fitting programs will also calculate a χ^2 or R^2, which are measures of how well the regression fits the actual data (the Goodness of Fit). These parameters assess the variation of the actual data from the fitted curve, and in general, a R^2 value close to 1 or a χ^2 value close 0 are taken as evidence that the data are fit well by the model. However, caution should be exercised in using these values since fitting data to the wrong model can still yield what appears to be a statistically "good fit". For those interested in learning more about the intricacies of curve fitting, there are many excellent publications, some of which are referenced here.[14,18−20]

■ ENZYME ASSAYS

Steady-State Enzyme Kinetics. Many drug targets are enzymes, and hence, SAR is commonly based on assays in which

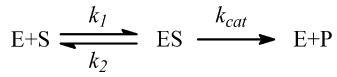

Figure 1. Kinetic scheme used to derive the Michaelis−Menten equation. k_1 is the rate constant for formation of ES from E + S; k_2 is the rate constant for the dissociation of ES back to E + S, and k_{cat} is the turnover number for the enzyme.

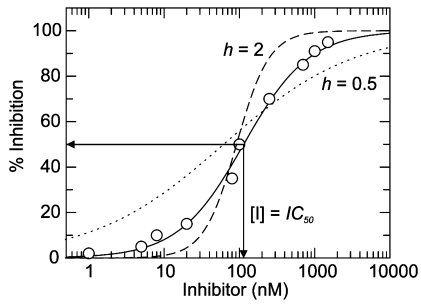

Figure 2. Determination of IC_{50} using a concentration−response equation. Data for inhibition of an enzyme-catalyzed reaction, determined by measuring initial velocities as a function of inhibitor concentration ([I]) with [I] ≫ [E], have been fit to an equation in which the response increases with [I] (eq 2) to give an IC_{50} of 114 nM. The data have been converted into % inhibition where the response changes from 0% to 100% inhibition over the experiment so that only 1 parameter is needed for initial data fitting, constraining the slope factor (Hill coefficient, h) to be 1. In a 2-parameter fit, h would be allowed to vary, while in a 4-parameter fit, the range over which the response varies (Y_{max} − Y_{min}) as well as the background signal (Y_{min}) are also variables (eq 3). Also shown are the calculated fits if h is constrained to 2 or 0.5, where it can be seen that there is a systematic deviation between the fitted curve and the experimental data points.

DOI: 10.1021/acsinfecdis.9b00012
ACS Infect. Dis. 2019, 5, 796−808

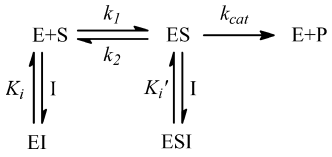

Figure 3. Competitive, noncompetitive/mixed, and uncompetitive inhibition. A competitive inhibitor binds to free enzyme and competes with the substrate while an uncompetitive inhibitor binds to the ES complex (binds after the substrate). A mixed inhibitor binds to both E and ES, while a pure noncompetitive inhibitor has equal affinity for E and ES ($K_i = K_i'$).

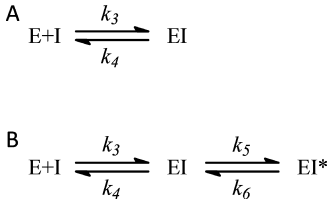

Figure 4. Slow-binding inhibition mechanisms. (A) A one-step mechanism. (B) A two-step mechanism in which the rapid formation of the initial EI complex is followed by a slow step leading to the final EI* complex. These are mechanisms A and B from Morrison and Walsh.[30] Note that by convention inhibition rate constants are numbered starting with k_3 since k_1 and k_2 are used to describe substrate binding (Figure 1).

the effect of compounds on the rate of substrate consumption or product formation is monitored. Consequently, it is worth reminding ourselves of approximations used in deriving the Michaelis Menten equation (eq 1), which is based on the simple reaction scheme shown in Figure 1; viz, (i) $[S] \gg [E]$ so that $[S]_{free} \approx [S]_{total}$, and (ii) initial velocity is determined in the first few % of the reaction so that $[S]$ is essentially constant.

$$v_i = \frac{V_{max}[S]}{K_m + [S]} \quad (1)$$

The Michaelis–Menten equation can be derived using the steady-state assumption in which the concentration of ES is assumed to be constant (cf. Briggs–Haldane derivation), and in eq 1, $V_{max} = k_{cat}[E]_{total}$, where $[E]_{total}$ is the total enzyme concentration and $K_m = (k_2 + k_{cat})/k_1$. K_m is the Michaelis–Menten constant and represents the dissociation constant of all enzyme bound species.

Basic Assumptions and Concentration (Dose)–Response Curves. Similar rate expressions can be derived to account for the impact of enzyme inhibitor on the rate of the reaction. In inhibition assays, it is also often assumed that $[I] \gg [E]$ again so that $[I]_{free} \approx [I]_{total}$ (see Box 2). This is because equilibrium constants are determined from the concentration of reactants present at equilibrium (i.e., $[S]_{free}$ or $[I]_{free}$), and given the above approximations, data analysis can use the total concentration of substrate or inhibitor added to the reaction.

Enzyme inhibition is most commonly analyzed using initial velocity measurements. Formally, the initial velocity is determined from a tangent to the initial portion of the reaction progress curve, and it is most convenient to use a continuous assay format so that the initial velocity can be accurately measured. However, many assays, including those run in high throughput, often rely on single time point or end point assays from which initial velocity data are extracted (see Box 2). In this case, it is important to recognize the underlying assumption that the reaction velocity is linear until the single time point is taken. If a continuous assay format is not available, we recommend that multiple time points are taken in order to check the linearity of the reaction. One simple control is to demonstrate that $v_i \propto [E]$, and thus, the initial velocity should double if the enzyme concentration is doubled.

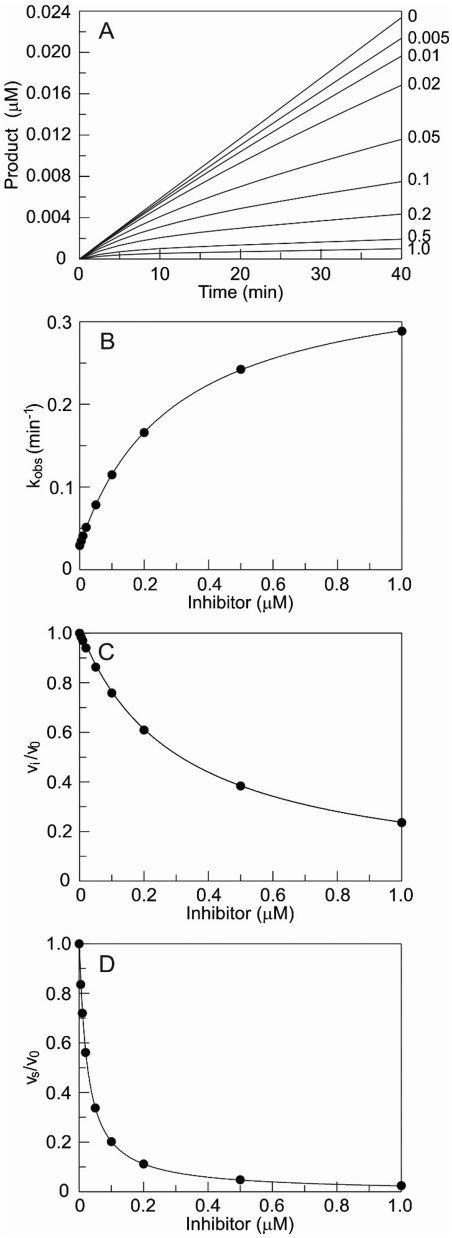

Figure 5. Progress curve analysis of a two-step slow-binding inhibitor. Under conditions where the reaction velocity is linear in the absence of inhibitor (v_0), curvature in the presence of inhibitor is diagnostic of slow-binding inhibition.[30] The figure shows forward progress curve analysis for the inhibition of an enzyme simulated using Kintek,[32] which follows a two-step induced fit mechanism in which the rapid formation of the initial enzyme–inhibitor complex (EI) is followed by the slow isomerization of EI to EI*. (A) Fitting of the data to the progress curve equation (eq 5) yields values for v_i, the initial velocity, v_s, the final steady-state velocity, and k_{obs}, the rate constant for formation of the steady state. (B) The hyperbolic dependence of k_{obs} on [I] is consistent with the two-step induced-fit mechanism and fitting of the data to eq 6 gives $k_5 = 0.34$ min^{-1}, $k_6 = 0.029$ min^{-1}, and $K_i^{app} = 0.34$ μM. (C) Consistent with a two-step mechanism, v_i varies with [I], and a fit of the data to eq 7 also gives a value for K_i^{app}. (D) A fit of v_s/v_0 against [I] to eq 8 gives $K_i^{*app} = 0.026$ μM.

DOI: 10.1021/acsinfecdis.9b00012
ACS Infect. Dis. 2019, 5, 796–808

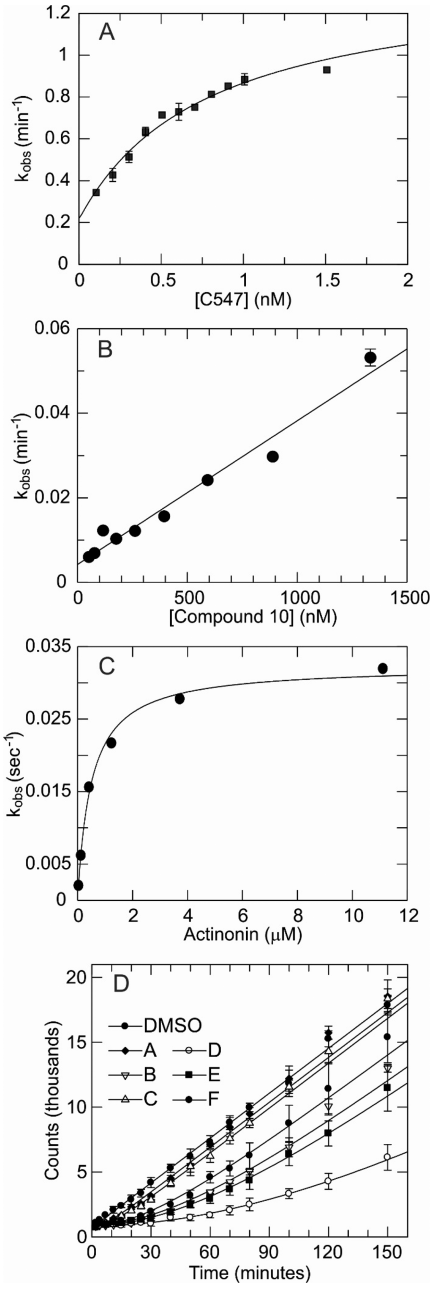

Figure 6. Examples of slow-binding inhibition analysis. (A) k_{obs} vs [I] plot for the slow-binding inhibition of acetylcholinesterase by C547, which follows a two-step binding mechanism. Adapted with permission from Kharlamova, A. D., Lushchekina, S. V., Petrov, K. A., Kots, E. D., Nachon, F., Villard-Wandhammer, M., Zueva, I. V., Krejci, E., Reznik, V. S., Zobov, V. V., Nikolsky, E. E., and Masson, P. (2016) Slow-binding inhibition of acetylcholinesterase by an alkylammonium derivative of 6-methyluracil: mechanism and possible advantages for myasthenia gravis treatment, *Biochem J. 473*, 1225−1236. DOI 10.1042/BCJ20160084. Copyright 2016 The Biochemical Society.[34] (B) k_{obs} vs [I] plot for the slow-binding inhibition of rhomboid protease GlpG by peptidyl ketoamide compound **10**, which follows a one-step binding mechanism. Adapted with permission from Ticha, A., Stanchev, S., Vinothkumar, K. R., Mikles, D. C., Pachl, P., Began, J., Skerle, J., Svehlova, K., Nguyen, M. T. N., Verhelst, S. H. L., Johnson, D. C., Bachovchin, D. A., Lepsik, M., Majer, P., and Strisovsky, K. (2017) General and Modular Strategy for Designing Potent, Selective, and Pharmacologically Compliant Inhibitors of Rhomboid Proteases, *Cell Chem. Biol. 24*, 1523−1536.e4. DOI 10.1016/j.chembiol.2017.09.007. Available under the terms of the Creative Commons Attribution License (CC BY).[35] (C) k_{obs} vs [I] plot for the slow-binding inhibition of polypeptide deformylase by actinonin, which follows a two-step binding mechanism. In this case, the intercept on the *Y*-axis is close to 0, and so, the data have been analyzed using a modified version of eq 6 where k_6 is set to 0. In this case, k_5 and K_i^{app} are actually k_{inact} and K_I, which are the parameters for quantifying irreversible enzyme inactivation (see below). Adapted from Van Aller, G. S., Nandigama, R., Petit, C. M., DeWolf, W. E., Jr., Quinn, C. J., Aubart, K. M., Zalacain, M., Christensen, S. B., Copeland, R. A., and Lai, Z. (2005) Mechanism of time-dependent inhibition of polypeptide deformylase by actinonin, *Biochemistry 44*, 253−260. DOI 10.1021/bi048632b. Copyright 2005 American Chemical Society.[36] (D) Jump-dilution progress curve analysis for the inhibition of LpxC by six inhibitors (A−F). Adapted with permission from Walkup, G. K., You, Z., Ross, P. L., Allen, E. K., Daryaee, F., Hale, M. R., O'Donnell, J., Ehmann, D. E., Schuck, V. J., Buurman, E. T., Choy, A. L., Hajec, L., Murphy-Benenato, K., Marone, V., Patey, S. A., Grosser, L. A., Johnstone, M., Walker, S. G., Tonge, P. J., and Fisher, S. L. (2015) Translating slow-binding inhibition kinetics into cellular and in vivo effects, *Nat. Chem. Biol. 11*, 416−423. DOI 10.1038/nchembio.1796. Copyright 2015 Springer Nature.[2]

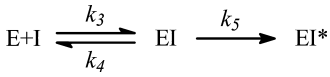

Figure 7. Two-step mechanism for irreversible inhibition. Reversible formation of the initial EI complex is followed by a second irreversible step leading to the covalent enzyme−inhibitor complex EI*. The kinetic mechanism is analogous to the reversible two-step mechanism in Figure 4 except that $k_6 = 0$. Irreversible inhibition is normally quantified by k_{inact}/K_I, the second order rate constant for the formation of EI*, where K_I is the concentration of inhibitor required to reach the half-maximal rate of inactivation of enzyme and k_{inact} is the maximum rate of inactivation at saturating inhibitor concentrations. Note that K_I is not the same as K_i, the equilibrium constant for dissociation of EI where $K_i = k_4/k_3$. While K_I can be numerically equal to K_i (e.g., when $k_4 \gg k_5$), this is often not the case. and k_{inact}/K_I should be used to quantify inhibitor potency.

The change in the initial velocity as a function of inhibitor concentration is then often fit to a concentration−response relationship to obtain the IC_{50} value for the inhibitor. Software programs, such as GraphPad Prism and GraFit, include several forms of the standard IC_{50} equation that differ depending on whether the response increases or decreases with inhibitor concentration and also whether the data are fit to a two or four parameter equation (eqs 2 and 3, respectively).

$$\%\,\text{inhibition} = \frac{100}{1 + \left(\frac{IC_{50}}{[I]}\right)^h} \quad (2)$$

$$Y = Y_{min} + \frac{Y_{max} - Y_{min}}{1 + \left(\frac{IC_{50}}{[I]}\right)^h} \quad (3)$$

In eqs 2 and 3, where the response is assumed to increase with [I], [I] is $[I]_{free}$, and h is the Hill coefficient or slope factor. Most programs set h as a variable in addition to IC_{50}. However, in a simple binding equilibrium, where there is no cooperativity and only 1 binding site, h is expected to be 1. It is thus recommended that h is set to 1 during data fitting and then allowed to float only if there is clear indication that the experimental data cannot be adequately modeled using $h = 1$, for example, if there is an obvious systematic deviation between the fitted curve and the experimental data. There are a number of mechanistic and artifactual reasons that can lead to values of h that deviate from

DOI: 10.1021/acsinfecdis.9b00012
ACS Infect. Dis. 2019, 5, 796−808

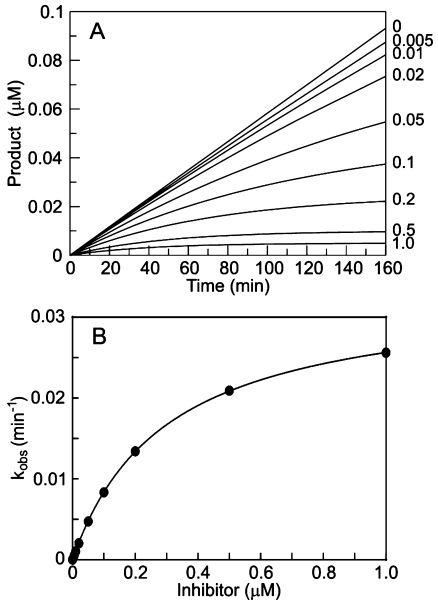

Figure 8. Irreversible inhibition. The kinetics for irreversible enzyme inhibition quantified by progress curve analysis. (A) Time-dependent enzyme inactivation as a function of inhibitor concentration (μM) has been analyzed using a simplified version of the progress curve equation (eq 9) since $k_6 = 0$, which yields values of k_{obs} and v_i as described in Figure 5.[12] (B) A plot of k_{obs} vs [I] is hyperbolic, consistent with a two-step mechanism in which the initial noncovalent association of the inhibitor with the enzyme is followed by a second-step leading to formation of the final covalent enzyme−inhibitor complex. Fitting of the data to eq 10 yields values for $k_{inact} = 0.033$ min^{-1}, $K_I^{app} = 0.28$ μM, and $k_{inact}/K_I^{app} = 0.12$ μM min^{-1}. Again, by analogy to equations for slow-binding inhibitors, eq 10 includes K_I^{app}, the apparent value for K_I, since the presence of substrate will affect the concentration of inhibitor required to reach $1/2k_{inact}$. Time-dependent enzyme inactivation was simulated using Kintek.[32]

unity,[12] for example, if there is positive ($h > 1$) or negative ($h < 1$) cooperativity or if the inhibitor operates through a nonspecific mode of action, e.g., due to aggregation.[21] In addition, if the potency of the inhibitor is underestimated, then the chosen enzyme concentration could result in $K_i/[E]_T$ ratios that result in tight binding inhibition ($K_i/[E]_T$ is between 10 and 0.01, Zone B, or <0.01, Zone C),[22] giving h values greater than 1. However, an explanation has to be proposed if h differs significantly from unity (see Box 2). For each IC_{50} determination, authors should show the concentration−response data and the fitted curve on a semilog plot either in the main text or in supporting information (see Box 1). In addition, the standard concentration−response equation often allows both the minimum and maximum values of the response to vary too, so that the data are fit to a four-parameter equation (four-parameter logistic) (eq 3, Y_{max}, Y_{min}, IC_{50}, and h). However, the use of a four-parameter fit implicitly assumes that enzyme inhibition does not vary from 0% to 100%, for example, that there is a background rate that is not affected by enzyme inhibition, and again, there has to be sound reasoning for increasing the number of parameters in the data analysis. In addition, the minimum rate cannot be less than the assay background rate and the maximum velocity cannot be greater than the uninhibited reaction velocity. Other experimental issues that may be encountered include solubility of the inhibitor, which may prevent 100% inhibition from being reached.

Figure 2 shows a typical concentration−response plot where the data have been fit to eq 2 and h has been constrained to 1. Also shown are the fits if h is constrained to 2 or to 0.5.

Box 2. Enzyme Assays and Concentration−Response Curves

(vi) When establishing assays, consider the methods that will be used to analyze the data. In many cases, data fitting assumes that $[I]_{free} \approx [I]_{total}$.
(vii) Single time point assays generally assume that the change in activity is linear with time, from the start of the reaction up until the time of measurement. Evidence should be provided that supports this assumption.
(viii) For coupled assays, check that the coupling enzyme is not rate-limiting and that your inhibitor is not inhibiting the coupling enzyme(s).
(ix) When fitting data to a concentration−response equation, use a two-parameter fit to obtain IC_{50} values and initially set $h = 1$. Provide a mechanistic hypothesis if h varies significantly from 1. In addition, if the data are fit using a four-parameter model, discuss the origin of, e.g., a background signal.
(x) In contrast to K_i values, IC_{50} values do not give information about the mechanism of inhibition. For instance, the observation of pure noncompetitive inhibition ($K_i = K_i'$) may be indicative of a promiscuous aggregator.
(xi) IC_{50} values depend on the precise experimental conditions that are used in the assay, such as enzyme and substrate concentration, and thus cannot be used to compare inhibition of a specific enzyme by different laboratories. In contrast, K_i values offer a more rigorous basis for comparison.
(xii) IC_{50} values can be converted to K_i values using the Cheng−Prusoff relationship *if* the mechanism of inhibition is known and also the $[S]/K_m$ ratio.

If there is no prior knowledge of compound potency, then it is not possible to choose appropriate inhibitor concentrations before any measurements have been made. In this case, it is recommended that the extent of inhibition is assessed using several fixed inhibitor concentrations that vary by factors of 10, say 0.1, 1, and 10 μM. Once it is possible to estimate concentrations that span a response from ~10% to 90% inhibition, it is then important to recognize that the level of inhibition is not a linear function of [I] (Figure 2), and thus, inhibitor concentrations should be chosen on the basis of a logarithmic rather than a linear scale to ensure an even distribution of data points across the plot. On a log scale, 3.16228 is halfway between 1 and 10, not 5. In addition, there should be enough data points at high and low concentrations to clearly define the end points for curve fitting. Finally, the pIC_{50} ($-\log_{10}(IC_{50})$) rather than the IC_{50} is sometimes reported to account for the exponential nature of the relationship.[23] It is important to realize that the IC_{50} value is a function of both the enzyme and substrate concentration. Thus, caution should be exercised when comparing IC_{50} values for the inhibition of a specific enzyme by different laboratories even when determined under "identical" conditions. K_i values, which do not depend on [E] or [S], offer a more rigorous basis for comparison.

Coupled Assays. Continuous assays often follow the change in a spectroscopic signal, such as the absorbance or fluorescence of the substrate or product, as a function of time. However, in situations where neither substrate nor product has a convenient spectroscopic signature, the enzyme reaction of interest may be coupled to a second reaction that does lead to change in signal that can be easily monitored. In this case, it is important to show that

DOI: 10.1021/acsinfecdis.9b00012
ACS Infect. Dis. 2019, 5, 796−808

the coupling reaction is not rate limiting and that the inhibitor does not affect the activity of the coupling enzyme (see Box 2). In addition, it is often not realized that there may be an initial lag in reaction velocity before the initial steady-state velocity is reached. The lag depends on factors such as the k_{cat} and K_m of the coupling enzyme and can be minimized by adjusting the concentration of the coupling enzyme.[24] If it is not possible to eliminate the lag phase by adjusting the assay conditions, then the initial velocities should be obtained after ensuring that the lag is complete.

K_i instead of IC_{50}. While concentration−response curves represent the bulk of activity measurements in SAR, enzyme inhibition can also be quantified by obtaining K_i values. This can be accomplished by determining k_{cat} and K_m values at different fixed inhibitor concentrations and using this information to generate K_i values, together with information on the mechanism of inhibition: competitive (K_i), noncompetitive/mixed (K_i and K_i'), and uncompetitive (K_i') (Figure 3). Although this is more laborious than an IC_{50} measurement, K_i values enable a better comparison of inhibitor potency between compounds since IC_{50} values depend on the precise experimental conditions that are used, such as substrate concentration, and provide no mechanistic information about the mode of inhibition (see Box 2). K_i values can be calculated from IC_{50} values using the Cheng−Prusoff relationship;[25] however, this requires knowledge of the mechanism of inhibition as well as the ratio of $[S]/K_m$. The mechanistic information derived from K_i measurements is useful since not all compounds are competitive inhibitors (although this is often assumed in the absence of any mechanistic data). In addition, the observation of pure noncompetitive inhibition ($K_i = K_i'$) may be indicative of a promiscuous inhibitor since it is highly unlikely that an inhibitor has equal affinity for both E and ES.[21,26] Furthermore, uncompetitive inhibition is often considered an advantage since the increase in substrate concentration caused by target inhibition will increase the level of inhibition rather than competing off the inhibitor.

Complexities: Tight Binding Inhibition. Tight binding inhibition occurs when the K_i value is similar to, or below, the enzyme concentration ($K_i/[E]_T < 10$), leading to depletion of the free inhibitor in the assay so that the assumption $[I]_{free} \approx [I]_T$ is no longer valid (see Box 3). It is thus an experimental definition since it is based on the lowest enzyme concentration that can be used in the assay. Clearly, this is a good problem to have, since we generally want compounds that are very potent. To account for inhibitor depletion under tight binding conditions, inhibition is quantified using the Morrison equation, which includes the total inhibitor concentration $[I]_T$ rather than the free concentration of inhibitor present at equilibrium ($[I]_{free}$) (eq 4).

Box 3. Tight Binding Inhibition

(xiii) If IC_{50} values start to approach $[E]$, tight binding inhibition may be occurring. In this case, IC_{50} measurements can seriously underestimate the potency of the compound. A valid IC_{50} value cannot be less than $1/2[E]$.

(xiv) Tight binding inhibition will lead to a depletion in the concentration of free inhibitor. This can be accounted for using the Morrison equation provided that $K_i/[E]_T > 0.01$.

$$\frac{v_i}{v_0} = 1 - \{(([E]_T + [I]_T + K_i^{app}) - \sqrt{([E]_T + [I]_T + K_i^{app})^2 - 4[E]_T[I]_T})/2[E]_T\} \quad (4)$$

For tight binding inhibitors, IC_{50} values can seriously underestimate potency and caution should be exercised if IC_{50} values start approaching $[E]$: note that the IC_{50} cannot be smaller than $1/2[E]$. Finally, if $IC_{50} < 1/2[E]$ is observed, then this could be because the concentration of active enzyme in the reaction has been overestimated. Indeed, it should be noted that use of the Morrison equation to determine K_i^{app} requires an accurate value for the enzyme concentration, unlike when $[I] \gg [E]$. If tight-binding is suspected, then IC_{50} values should be determined at more than one enzyme concentration: If $[I] \gg [E]$, then the IC_{50} value will not change if the enzyme concentration is altered; however, the IC_{50} value will change for a tight binding inhibitor and indeed plotting IC_{50} against $[E]$ should yield a straight line with a Y-intercept where $IC_{50} = K_i^{app}$.

Complexities: Slow-Binding Inhibition. In addition to assumptions such as $[S] \gg [E]$ and $[I] \gg [E]$, it is also often assumed that the system rapidly reaches equilibrium (i.e., in the mixing time of the experiment). However, some compounds are slow-binding inhibitors in which the steady state is reached slowly on the time scale of the assay that is used (see Box 4). Slow-binding inhibitors will also dissociate slowly from their targets, which has important pharmacological consequences since the time scale for breakdown of the drug−target complex can be on the same time scale as the rate of drug elimination.[27−29] Slow-binding inhibition can occur via several mechanisms; however, the most commonly encountered are a one-step mechanism or a two-step mechanism in which the rapid formation of the initial enzyme−inhibitor complex is followed by a slow step leading to the final enzyme−inhibitor complex (Figure 4).

Slow-binding inhibition can be diagnosed by observing curvature in the enzyme assay under conditions where the uninhibited reaction is linear, and data are often analyzed by forward or reverse (jump dilution) progress curves (see Box 4). Figure 5 contains forward progress curve data for the inhibition of an enzyme by a time-dependent inhibitor. The progress curves are fit to eq 5 giving values for v_i, v_s, and k_{obs} as a function of $[I]$, where v_i is the initial velocity in the presence of the inhibitor, v_s is the final steady-state velocity, and k_{obs} is the rate constant for onset of inhibition. The dependence of k_{obs} on $[I]$ can be used to distinguish between one- and two-step mechanisms: in this case, the plot is hyperbolic, consistent with an induced-fit two-step mechanism (Mechanism B), and a fit of the data to eq 6 gives values for k_5 and k_6 (Figure 4) as well as K_i^{app}, the dissociation constant of EI. K_i^{app} can also be extracted directly from a plot of v_i/v_0 against $[I]$ (eq 7), where v_0 is the rate in the absence of the inhibitor, while K_i^{*app}, the overall dissociation constant, can be obtained by fitting the dependence of v_s/v_0 on $[I]$ to eq 8. In a one-step mechanism, v_i does not vary with $[I]$.[31]

Note that in these equations we use K_i^{app} and K_i^{*app}, the apparent values for the equilibrium dissociation constants. This is because progress curve analysis is performed at a single substrate concentration, which is often very high to ensure that the velocity in the absence of inhibitor is linear. Thus, the experimentally measured dissociation constant will depend on the amount of enzyme that is present as ES (see Box 4). The true values for the equilibrium constants can be obtained from the apparent values using the Cheng−Prusoff equation if both the mechanism of inhibition is known as well as the value for the substrate K_m. For example, if $[S] > K_m$ then K_i^{app} will be larger than K_i by a ratio of $1 + [S]/K_m$ for a competitive inhibitor. Analogous correction factors are also available for noncompetitive and uncompetitive inhibitors.

DOI: 10.1021/acsinfecdis.9b00012
ACS Infect. Dis. 2019, 5, 796−808

Box 4. Slow and Irreversible Inhibition

(xv) Check for time-dependent effects in binding/inhibition. IC_{50} shifts following preincubation of enzyme and inhibitor before initiating the reaction by addition of substrate can be used to check for slow-binding inhibition, but this only works for an inhibitor that binds in the absence of the substrate. In addition, the decrease in activity following preincubation could have other explanations, for example, that the inhibitor is causing the enzyme to denature.

(xvi) Slow-binding inhibition can often be diagnosed by observing curvature in reaction progress curves under conditions where the reaction in the absence of inhibitor is linear. However, it is important to show that curvature does not result from instability of the enzyme under the assay conditions. In addition, linearity may only be accomplished by using high concentrations of substrate, and thus, the apparent dissociation constants obtained under the specific assay conditions (K_i^{app} and K_i^{*app}) may differ significantly from the true values as described by the Cheng−Prusoff equations.

(xvii) Slow-binding inhibition can occur by both one- and two-step mechanisms, but the ability to distinguish these two mechanisms may be affected by inhibitor solubility and/or the dissociation constant of the first step in a two-step mechanism. For example, a linear increase in k_{obs} as a function of [I] is consistent with a one-step mechanism. However, this plot can also be linear for a two-step mechanism if the highest inhibitor concentration that is used does not saturate the enzyme (i.e., $[I] < K_i^{app}$).

(xviii) If the off-rate (k_4 or k_6) is very slow, then the intercept on the *Y*-axis of the k_{obs} vs [I] plot may be close to 0, and thus, it may be difficult to distinguish reversible slow-binding inhibition from irreversible inhibition. Additional methods may then be needed to verify that the inhibition is indeed irreversible and/or to quantify the off-rate for very slowly dissociating compounds.

(xix) For compounds that bind very slowly, it may be easier to use reverse progress curve analysis (jump dilution), where enzyme and inhibitor are preincubated prior to dilution into the reaction solution.[2]

(xx) Tight-binding inhibition may occur with very potent compounds, requiring data analysis that is based on $[I]_{total}$ rather than $[I]_{free}$ as described by the Morrison equation.

(xxi) SKR for irreversible inhibition should use k_{inact}/K_I and not IC_{50} values.

$$[P] = v_s t + \frac{v_i - v_s}{k_{obs}}(1 - e^{(-k_{obs}t)}) \quad (5)$$

$$k_{obs} = k_6 + \left(\frac{k_5}{1 + K_i^{app}/[I]}\right) \quad (6)$$

$$\frac{v_i}{v_0} = \frac{1}{1 + ([I]/K_I^{app})} \quad (7)$$

$$\frac{v_s}{v_0} = \frac{1}{1 + ([I]/K_I^{*app})} \quad (8)$$

Several challenges exist in analyzing slow-binding inhibitors. For example, it may be difficult, due to issues such as substrate solubility, cost, or availability, to achieve reaction conditions where the initial velocity in the absence of inhibitor is linear for sufficient time to observe curvature in the presence of inhibitor. In addition, it may be difficult to distinguish one- and two-step binding mechanisms. For example, if the initial binding event in a two-step mechanism has a relatively high K_i^{app}, then it may be difficult to reach sufficient inhibitor concentration to observe curvature in the k_{obs} vs [I] plot. In this case, a two-step binding mechanism can give the appearance of a one-step mechanism. Note that for two-step binding, v_i is also expected to vary with [I] (Figure 5C); however, this may also be difficult to detect for the same reason. Finally, if the rate of dissociation of inhibitor from the enzyme is very slow, then it may be difficult to distinguish reversible from irreversible inhibition since the intercept on the *Y*-axis of the k_{obs} vs [I] plot will be close to 0 (see Box 4). For reversible inhibitors with slow off-rates, it may be easier to perform a jump dilution (reverse progress curve) assay, in which enzyme and inhibitor are preincubated for several hours before dilution into a reaction mixture containing substrate. In this case, the reaction velocity will increase as the inhibitor slowly dissociates from enzyme leading to a reverse progress curve. For slowly dissociating inhibitors, it may also be possible to prepare and purify the enzyme−inhibitor complex and then directly monitor the rate of inhibitor dissociation after diluting the complex. For high affinity inhibitors, it will be necessary to use a very sensitive method to quantify free inhibitor concentration such as mass spectrometry or radioactivity.[33] Several examples of the above scenarios are shown in Figure 6.

Complexities: Irreversible Inhibition. Irreversible inhibitors are compounds that bind to the target and do not dissociate. As noted above, some slow-binding inhibitors, including those that form a covalent complex with the target as well as those that are noncovalently bound, can appear to be irreversible if the off-rate is very slow. In this situation, it is important to perform additional assays to determine whether the compounds are indeed reversible, such as jump dilution assays to check for reactivation of the enzyme. While it is tempting to use IC_{50} measurements to quantify the "potency" of irreversible inhibitors, such experiments are flawed since they cannot account for the time dependence of inhibition and virtually any IC_{50} can be achieved if the reaction is allowed to incubate for long enough. Instead, it is more appropriate to determine k_{inact}/K_I, which is the second order rate constant for formation of the irreversible enzyme−inhibitor complex (see Box 4). Irreversible inhibitors often operate through a two-step mechanism in which the inhibitor first binds reversibly to the enzyme followed by covalent bond formation (Figure 7).

Analysis of irreversible inhibition follows a similar approach to that used for slow-binding inhibitors except that a simplified progress curve equation can be used since $k_6 = 0$ and $v_s = 0$ (eq 9). Simulated data are shown in Figure 8 where it can be seen that the appearance of the plots is very similar to those for two-step slow-binding reversible inhibition except that the intercept of the k_{obs} vs [I] plot passes through 0. In addition, v_s values will have a finite value for reversible inhibitors whereas v_s values obtained from forward progress curves should tend to 0.

$$[P] = \frac{v_i}{k_{obs}}(1 - e^{(-k_{obs}t)}) \quad (9)$$

$$k_{obs} = \frac{k_{inact}}{1 + (K_I^{app}/[I])} \quad (10)$$

DOI: 10.1021/acsinfecdis.9b00012
ACS Infect. Dis. 2019, 5, 796−808

If the initial binding event is weak, then it may not be possible to saturate the enzyme in order to determine values for k_{inact} and K_I^{app} individually. In this case, the plot of k_{obs} vs [I] will be linear with a slope of k_{inact}/K_I^{app}. An interesting recent example of this behavior is the covalent inhibition of $KRAS^{G12C}$ by compounds that bind weakly (K_i > 64 μM) but react rapidly with C12 (k_{inact} > 0.019 s^{-1}).[37]

DIRECT BINDING ASSAYS

Binding kinetics can also be determined using approaches that directly measure the formation and breakdown of the drug−target complex. These assays are used when no functional assay is available or when binding of ligands to the free enzyme is being assessed. Numerous methods are available, including the use of radiolabeled compounds and mass spectrometry, which provide the highest levels of sensitivity, to approaches in which there is a change in spectroscopic signal on binding. In many cases, the analysis of data from direct-binding assays depends on the same fundamental principles and assumptions described for enzyme assays. Below, I briefly discuss several methods that are in common use.

Radioligand Binding Assays. Receptor−ligand binding assays have historically relied on the use of radiolabeled ligands, which permit binding to be measured for purified receptors or receptors on cell surfaces.[38,39] In these assays, the concentration of bound ligand is often determined directly after free ligand is removed from an immobilized receptor preparation using a wash step (often performed with cold buffer). This approach assumes that the wash step is fast relative to the rate of ligand dissociation. In addition, it is important to vary incubation times to ensure that the system is at equilibrium and also to account for nonspecific binding. Data analysis often assumes that the concentration of receptor ([R]) is very low so that [L] ≫ [R] at every concentration of ligand ([L]) and thus that $[L]_{free} \approx [L]_{total}$ (see Box 5). However, if $K_d/[R] < 10$ then ligand depletion will occur, and the quadratic Morrison equation must be used, with the caveat that the concentration of receptor is accurately known. Finally, a simple one-site binding event should have a Hill slope (h) of 1. Once a radioligand binding assay has been developed, then the binding of additional ligands can be measured using a competitive radioligand binding assay. This can be performed under equilibrium conditions to obtain the K_d for binding but can also be adapted, as described by Motulsky and Mahan, to provide the on- and off-rates for ligand binding.[1,40]

Box 5. Direct Binding Assays

(xxii) Many direct binding assays have the same assumptions as those used for activity measurements, for example, that $[L]_{free} \approx [L]_{total}$.

(xxiii) Competitive radioligand or fluorescence-based assays are often used to assess the binding of other ligands. Generally, it is advisable to first quantify the binding of the competitor on its own in order to reduce the number of variables in fitting data obtained from the competition assay.

(xxiv) Data obtained by methods such as SPR or ITC will usually be analyzed by software provided with the instruments. While this is convenient, investigators should determine what assumptions have been made in deriving the mathematical models that are used for data analysis.

Fluorescence Binding Assays. Many direct binding assays are based on a change in spectroscopic signal upon formation of the receptor−ligand complex. This includes methods in which the fluorescence of the protein and/or ligand is altered. The change in fluorescence is determined as a function of ligand concentration, and the K_d for the ligand is obtained by fitting the data to a binding isotherm using equations described above where the same assumptions, such as [L] ≫ [R], may apply (see Box 5). Again, it is suggested that h is set to 1 for initial data fitting. Fluorescence-based methods are generally less sensitive than techniques based on radioactivity or mass spectrometry, with a typical detection limit of ~10^{-8} M, although there are examples of assays where fluorescence and radiolabeling perform similarly.[3] Important experimental considerations include the need to account for the inner filter effect, in which the fluorophore is sufficiently concentrated to attenuate the excitation light and may also reabsorb some of the emitted light. In addition, while binding assays with radiotracers of known specific activity can give the absolute concentration of the receptor, the relative change in fluorescence intensity at saturation often cannot be directly related to concentration.

If there is no change in ligand fluorescence upon binding, the anisotropy or polarization may still be affected on complex formation due to a decrease in the rate of tumbling. Indeed, a common approach to the development of a binding assay is to append a fluorophore onto a ligand in a way that is not anticipated to perturb binding and then to use steady-state and time-resolved anisotropy measurements to quantify binding. A second common fluorescence-based assay is to attach a second fluorophore to the protein and use Förster/fluorescence resonance energy transfer (FRET) to monitor binding using either a steady-state or time-resolved detection.[41] FRET and methods such as bioluminescence resonance energy transfer (BRET) have been translated to quantifying drug−target interactions in living cells, such as by tagging the target with NanoLuc luciferase and monitoring BRET to a fluorescent ligand (NanoBRET).[7,42] Using a fluorescent competitor ligand, NanoBRET and other proximity-based assays can be used to assess binding of unlabeled ligands in an analogous approach to the competitive radioligand binding assay described above. When a competition assay is used, it is advisable to accurately determine the binding of the competitor so that the kinetic parameters for association and dissociation of the competitor are not also variables in fitting the competition binding data.

BIOLUMINESCENT REPORTER ASSAYS

In addition to bioluminescence resonance energy transfer (BRET), luciferases have found wide application in cell-based genetic reporter assays in which regulatory elements that control gene transcription are coupled to luciferase gene expression. This approach has proved particularly useful for drug targets such as GPCRs and nuclear hormone receptors, which regulate gene transcription. Andruska et al. report an HTS to discover inhibitors of 17β-estradiol (E2)−estrogen receptor α (ERα) induced breast cancer cell proliferation,[43] using a luciferase reporter whose expression is driven by three copies of the consensus estrogen response element $(ERE)_3$. The authors discuss compounds that show activity in the primary screen due to a direct effect on luciferase or that are broadly cytotoxic, in addition to compounds that affect cell proliferation through inhibition of ERα.

Surface Plasmon Resonance and Isothermal Titration Calorimetry. Biophysical methods play a major role in characterizing the structure, kinetics, and thermodynamics of

DOI: 10.1021/acsinfecdis.9b00012
ACS Infect. Dis. 2019, 5, 796−808

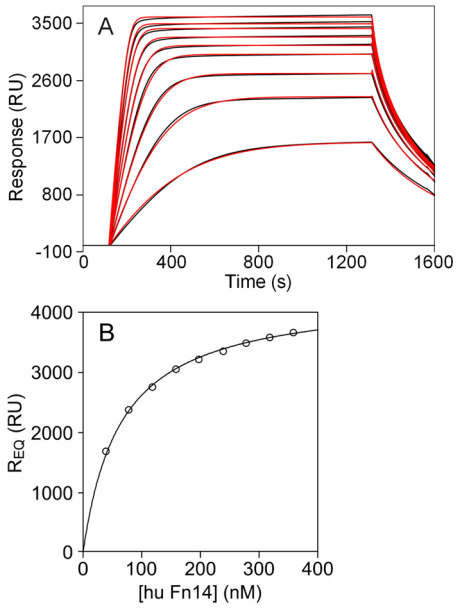

Figure 9. SPR sensorgram. Biacore analysis of soluble monomeric TNF family receptor Fn14 binding to the TNF family ligand TWEAK. (A) Sensorgram for 40−360 nM soluble receptor binding to surface derivatized with TWEAK. The experimental data (black lines) were globally fit to a 1:1 binding model (red lines) using BIAevaluation to determine kinetic rate constants. (B) The signal observed at equilibrium, R_{EQ}, plotted as a function of soluble receptor concentration, fit to a hyperbolic, single-site binding equation. Adapted from Day, E. S., Cote, S. M., and Whitty, A. (2012) Binding efficiency of protein−protein complexes, *Biochemistry 51*, 9124−9136. DOI 10.1021/bi301039t. Copyright 2012 American Chemical Society.[45]

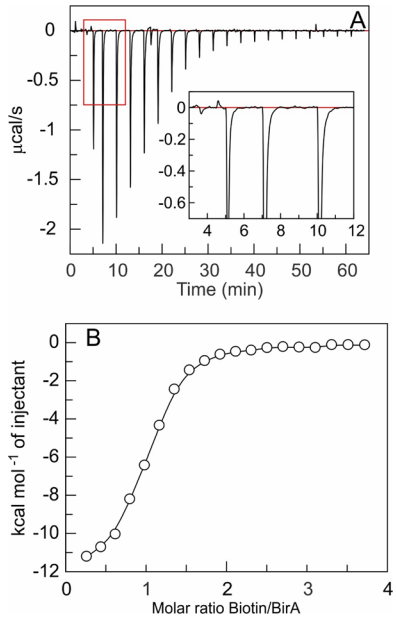

Figure 10. Binding of biotin protein ligase A (BirA) and biotin analyzed by ITC. (A) Raw calorimetric data obtained by the titration of biotin (900 μM) into wild type BirA (50 μM) at 25 °C in 10 mM Tris-HCl buffer (pH 7.5) containing 30 mM NaCl, 200 mM KCl, and 2.5 mM $MgCl_2$. Inset: Enlarged area of the titration curve showing that the system is at equilibrium before each injection. (B) The integrated heats of injection plotted as a function of the biotin/BirA molar ratio, fit to a single binding site model using Microcal Origin software after correcting for the heat of dilution to give $n = 0.981 \pm 0.007$, $K_a = 3.6 \times 10^5 \pm 2.0 \times 10^4$ M^{-1} ($K_d = 2.8$ μM), $\Delta H = -12.2 \pm 0.1$ kcal/mol, and $\Delta S = -15.3$ cal/mol/deg. Adapted from Bockman, M. R., Engelhart, C. A., Dawadi, S., Larson, P., Tiwari, D., Ferguson, D. M., Schnappinger, D., and Aldrich, C. C. (2018) Avoiding Antibiotic Inactivation in *Mycobacterium tuberculosis* by Rv3406 through Strategic Nucleoside Modification *ACS Infect. Dis.*, *4*, 1102−1113. DOI: 10.1021/acsinfecdis.8b00038. Copyright 2018 American Chemical Society.[54]

biomolecular interactions. While techniques such as X-ray crystallography and NMR spectroscopy are primarily used to provide insight into the structure of protein−ligand complexes, surface plasmon resonance (SPR) and isothermal titration calorimetry (ITC) are both label free approaches to quantifying protein−protein and protein−ligand interactions.[44] There are many excellent papers on the application of both SPR and ITC to the analysis of biomolecular interactions, and I only mention them here to draw the reader's attention to these methods. In SPR, one of the binding components is tethered to a surface and the change in SPR signal caused by the interaction with the second component yields both the thermodynamic and kinetic parameters for the interaction.[9] An example of a protein−protein interaction quantified by SPR is shown in Figure 9.[45] In addition to being label free, SPR can be deployed in relatively high throughput and is heavily used in the pharmaceutical industry for drug discovery campaigns. Experimental caveats include the ability to stably immobilize one of the binding partners and to then regenerate the surface after each binding reaction, and mass transfer effects that can mask the actual binding reaction, for example, if the transfer of the analyte from bulk solution to the sensor surface is slower than the binding event.[46,47] In addition, the tethered protein can also have different properties compared to the untethered protein in solution, which may alter ligand binding. HTS libraries invariably contain compounds, such as promiscuous aggregators, that give false hits due to assay interference,[26] and Giannetti et al. give clear examples of sensorgrams that arise from nonideal binding events caused by such compounds.[48] One interesting recent advance is the development of a "chaser" method that improves the ability of SPR to accurately quantify the kinetics of slowly dissociating ligands and thus overcome problems associated with signal drift.[8]

ITC is a solution-based method in which the heat liberated (exothermic) or absorbed (endothermic) by the binding event is used to measure thermodynamic binding parameters such as K_d, ΔH, and ΔS (Figure 10).[49] In contrast to SPR, ITC measures the binding reaction in solution, thus avoiding immobilization of a binding partner, but also usually requires larger amounts of sample and has lower throughput. One important aspect of ITC assay design is to minimize heat changes caused by mixing the solutions that contain the protein (cell) and analyte (syringe), and thus, it is desirable to dissolve both components in identical buffer solutions. It is also important to ensure that there is sufficient time between each injection so that the system can come to equilibrium. Errors in concentration of the protein will impact the stoichiometry (n), while errors in the concentration of the analyte will affect n, K_d, and ΔH.[50] In addition, concentrations should be chosen so that $n \times [\text{protein}]/K_d = 10-50$; however, meeting this requirement for either very high or low affinity ligands may be challenging. For example, high affinity ligands will require low protein concentrations, which will result in small changes in the amount of heat absorbed or released for each injection, which may be difficult to measure. Conversely, weak binders will require high concentrations of both protein and analyte, which may be difficult to attain due to solubility and/or availability of reagents. While ITC can quantify interactions over a range of affinities from nM to

DOI: 10.1021/acsinfecdis.9b00012
ACS Infect. Dis. 2019, 5, 796−808

sub-mM, this range depends on the absolute heat change and can be extended by using a competitive ligand.[51] Finally, although ITC is used almost exclusively for equilibrium binding measurements, there are reports that this method can also yield the kinetic parameters for binding.[52,53]

Both methods require specialized equipment, and in each case, the software that controls the instrument also includes curve fitting programs to analyze the data. Following the theme of this Perspective, investigators are urged not to treat the packaged data analysis programs as black boxes for data fitting but instead to understand which equations are being fitted to the data and what, if any, assumptions are made in this procedure (see Box 5). In SPR, curve fitting of the sensorgrams will yield the on- and off-rates for ligand binding, which are then used to calculate a K_d value. However, K_d values can also be calculated directly by plotting the signal at steady state (Response, RU) as a function of ligand concentration provided that the injection time is sufficiently long for the system to reach steady state.[55] In ITC, the binding isotherm is generated by plotting the amount of heat released or absorbed in each analyte injection as a function of analyte concentration. Curve fitting then yields n (stoichiometry), K_a (association binding constant where $K_a = 1/K_d$), and ΔH, from which ΔS and ΔG are calculated.[56] Initial curve fitting often assumes a 1:1 binding interaction in which case a value of $n = 1$ is expected. However, as noted above, n can often deviate from 1 due to inaccuracies in either the protein or ligand concentration.

SUMMARY: GUIDELINES FOR PUBLICATION OF QUANTITATIVE INHIBITION/BINDING DATA

In summary, many methods are available for quantifying biomolecular interactions. The choice of method will depend on the specific system under investigation, and in this Perspective, I have only attempted to highlight some of the most common approaches in order to draw attention to key experimental considerations, and also common problems (see Box 6), that are encountered in developing assays and analyzing the data that are produced. Instruments such as those used for SPR and ITC measurements come with their own software for analyzing the binding data, and while I have not attempted to describe the mathematical models used for these approaches, users should be aware of the underlying assumptions used here too.

AUTHOR INFORMATION

Corresponding Author

*E-mail: peter.tonge@stonybrook.edu. Tel: (631) 632-7907.

ORCID

Peter J. Tonge: 0000-0003-1606-3471

Notes

The author declares the following competing financial interest(s): Peter Tonge is a Founder of Chronus Pharmaceuticals Inc.

ACKNOWLEDGMENTS

This work was supported by grants from the National Institutes of Health (GM102864, EB024549, EB027050), the National Science Foundation (MCB1817837), and a PhRMA Foundation Fellowship.

ABBREVIATIONS

BRET, bioluminescence resonance energy transfer; FRET, Förster/fluorescence resonance energy transfer; h, Hill coefficient; IC_{50}, concentration of inhibitor (ligand) that results in 50% inhibition (effect); ITC, isothermal titration calorimetry; SKR, structure−kinetic relationship; SPR, surface plasmon resonance

Box 6. Common Problems

(xxv) The observation of a background rate (drift) before all the reagents have been combined could have several explanations including instrument drift, reagent instability, or changes in reagent solubility. It can be useful to scan the UV−vis spectrum of the reagent since precipitation will lead to light scattering, which will manifest as an increase in absorption across the whole absorbance spectrum, increasing as the wavelength decreases (since scattering intensity $\propto \lambda^{-4}$). Proteins and other reagents can also bind to surfaces, leading to changes in the effective concentration in solution. One useful control is to double [E] and show that the observed rate doubles. This is a good check that the change in signal is due to the enzyme catalyzed reaction.

(xxvi) Systematic errors in replicates could be due to reagent instability, and it is important to stagger replicates over the whole course of an experiment (e.g., at several times during the day) to check for systematic changes in activity. Proteins with essential Cys residues can lose activity due to oxidation, and reducing reagents (such as DTT) are often added to stock solutions or assays. Controls should be performed to check that the reducing reagent does not react with other reagents. The oxidized forms of some reducing reagents can have absorbance at 280 nm, so the background absorbance of a buffer containing DTT can increase slowly with time. Ligands (inhibitors) can also be unstable, especially if they contain reactive groups and/or aggregate or precipitate either before or after being added to the assay.

(xxvii) IC_{50} values less the 1/2[E] could occur if the enzyme is less active than assumed, for example, if it is not pure or if a fraction of the enzyme is inactive (e.g., due to oxidation; see above).

(xxviii) There can be several mechanistic or artifactual explanations for concentration−response plots with Hill coefficients (h) differing from unity. For instance, compounds that form colloidal aggregates will likely inhibit enzymes through a nonspecific mode of action, which often manifests as a steep response ($h > 1$). Feng and Shoichet have suggested a number of approaches to test for promiscuous inhibition.[58]

(xxix) Tight binding inhibition will also result in concentration−response plots with $h > 1$ and can have important consequences on the use of IC_{50} values for establishing SAR. Since $IC_{50} \geq 1/2[E]$, the dynamic range of SAR resulting from IC_{50} values is limited by the enzyme concentration, and thus, IC_{50} values can seriously underestimate compound potency (see discussion in Chapter 7, Tight Binding Inhibition, of Copeland[12]). Assuming that the assay has not bottomed-out, repeating the IC_{50} measurement at a lower enzyme concentration can be informative. For instance, if tight binding conditions are present, then reducing [E] will lead to a reduction in the apparent IC_{50} and a decrease in h values toward 1. This limitation in IC_{50} values again reinforces the benefit of determining K_i values.

DOI: 10.1021/acsinfecdis.9b00012
ACS Infect. Dis. 2019, 5, 796−808

REFERENCES

(1) Motulsky, H. J., and Mahan, L. C. (1984) The kinetics of competitive radioligand binding predicted by the law of mass action. *Mol. Pharmacol. 25*, 1−9.

(2) Walkup, G. K., You, Z., Ross, P. L., Allen, E. K., Daryaee, F., Hale, M. R., O'Donnell, J., Ehmann, D. E., Schuck, V. J., Buurman, E. T., Choy, A. L., Hajec, L., Murphy-Benenato, K., Marone, V., Patey, S. A., Grosser, L. A., Johnstone, M., Walker, S. G., Tonge, P. J., and Fisher, S. L. (2015) Translating slow-binding inhibition kinetics into cellular and in vivo effects. *Nat. Chem. Biol. 11*, 416−23.

(3) Handl, H. L., Vagner, J., Yamamura, H. I., Hruby, V. J., and Gillies, R. J. (2005) Development of a lanthanide-based assay for detection of receptor-ligand interactions at the delta-opioid receptor. *Anal. Biochem. 343*, 299−307.

(4) Zwier, J. M., Roux, T., Cottet, M., Durroux, T., Douzon, S., Bdioui, S., Gregor, N., Bourrier, E., Oueslati, N., Nicolas, L., Tinel, N., Boisseau, C., Yverneau, P., Charrier-Savournin, F., Fink, M., and Trinquet, E. (2010) A fluorescent ligand-binding alternative using Tag-lite(R) technology. *J. Biomol. Screening 15*, 1248−59.

(5) Wilson, D. J., Shi, C., Duckworth, B. P., Muretta, J. M., Manjunatha, U., Sham, Y. Y., Thomas, D. D., and Aldrich, C. C. (2011) A continuous fluorescence displacement assay for BioA: an enzyme involved in biotin biosynthesis. *Anal. Biochem. 416*, 27−38.

(6) Rinken, A., Lavogina, D., and Kopanchuk, S. (2018) Assays with Detection of Fluorescence Anisotropy: Challenges and Possibilities for Characterizing Ligand Binding to GPCRs. *Trends Pharmacol. Sci. 39*, 187−199.

(7) Stoddart, L. A., Kilpatrick, L. E., and Hill, S. J. (2018) NanoBRET Approaches to Study Ligand Binding to GPCRs and RTKs. *Trends Pharmacol. Sci. 39*, 136−147.

(8) Quinn, J. G., Pitts, K. E., Steffek, M., and Mulvihill, M. M. (2018) Determination of Affinity and Residence Time of Potent Drug-Target Complexes by Label-free Biosensing. *J. Med. Chem. 61*, 5154−5161.

(9) Cooper, M. A. (2002) Optical biosensors in drug discovery. *Nat. Rev. Drug Discovery 1*, 515−28.

(10) Yu, H., Dranchak, P., Li, Z., MacArthur, R., Munson, M. S., Mehzabeen, N., Baird, N. J., Battalie, K. P., Ross, D., Lovell, S., Carlow, C. K., Suga, H., and Inglese, J. (2017) Macrocycle peptides delineate locked-open inhibition mechanism for microorganism phosphoglycerate mutases. *Nat. Commun. 8*, 14932.

(11) Motulsky, H. J., and Ransnas, L. A. (1987) Fitting Curves to Data Using Nonlinear-Regression - a Practical and Nonmathematical Review. *FASEB J. 1*, 365−374.

(12) Copeland, R. A. (2013) *Evaluation of enzyme inhibitors in drug discovery: a guide for medicinal chemists and pharmacologists*, 2nd ed., Wiley, Hoboken, NJ.

(13) Sittampalam, G. S., Coussens, N. P., Brimacombe, K., Grossman, A., Arkin, M., Auld, D., Austin, C., Baell, J., Bejcek, B., Chung, T. D. Y., Dahlin, J. L., Devanaryan, V., Foley, T. L., Glicksman, M., Hall, M. D., Hass, J. V., Inglese, J., Iversen, P. W., Kahl, S. D., Kales, S. C., Lal-Nag, M., Li, Z., McGee, J., McManus, O., Riss, T., Trask, O. J., Jr., Weidner, J. R., Xia, M., and Xu, X., Eds. (2004) *Assay Guidance Manual*, Eli Lilly & Company and the National Center for Advancing Translational Sciences, Bethesda, MD.

(14) Motulsky, H. J., and Christopoulos, A. (2004) *Fitting Models to Biological Data Using Linear and Nonlinear Regression: A Practical Guide to Curve Fitting*, Oxford University Press, New York, NY, USA.

(15) Division of Biomedical Research Workforce National Institutes of Health. *Requirement for Instruction in the Responsible Conduct of Research*, https://grants.nih.gov/grants/guide/notice-files/NOT-OD-10-019.html.

(16) Blainey, P., Krzywinski, M., and Altman, N. (2014) Points of significance: replication. *Nat. Methods 11*, 879−880.

(17) Vaux, D. L., Fidler, F., and Cumming, G. (2012) Replicates and repeats–what is the difference and is it significant? A brief discussion of statistics and experimental design. *EMBO Rep. 13*, 291−6.

(18) Cornish-Bowden, A. (2014) Analysis and interpretation of enzyme kinetic data. *Perspectives in Science 1*, 121−125.

(19) Motulsky, H. J. *GraphPad Statistics Guide*, http://www.graphpad.com/guides/prism/7/statistics/index.htm.

(20) Vaux, D. L. (2012) Research methods: Know when your numbers are significant. *Nature 492*, 180−181.

(21) McGovern, S. L., Caselli, E., Grigorieff, N., and Shoichet, B. K. (2002) A common mechanism underlying promiscuous inhibitors from virtual and high-throughput screening. *J. Med. Chem. 45*, 1712−22.

(22) Straus, O. H., and Goldstein, A. (1943) Zone behavior of enzymes: illustrated by the effect of dissociation constant and dilution on the system cholinesterase-physostigmine. *J. Gen. Physiol. 26*, 559−585.

(23) Navare, M. *Use pIC50 Instead of IC50 to Think About Your Assays Logarithmically*, https://www.collaborativedrug.com/using-pic50-instead-of-ic50-will-change-the-way-you-see-your-drug-discovery-data/.

(24) Copeland, R. A. (2000) *Enzymes: a practical introduction to structure, mechanism, and data analysis*, 2nd ed., Wiley, New York.

(25) Cheng, Y., and Prusoff, W. H. (1973) Relationship between the inhibition constant (K1) and the concentration of inhibitor which causes 50% inhibition (I50) of an enzymatic reaction. *Biochem. Pharmacol. 22*, 3099−3108.

(26) Aldrich, C., Bertozzi, C., Georg, G. I., Kiessling, L., Lindsley, C., Liotta, D., Merz, K. M., Jr., Schepartz, A., and Wang, S. (2017) The Ecstasy and Agony of Assay Interference Compounds. *ACS Med. Chem. Lett. 8*, 379−382.

(27) Tonge, P. J. (2018) Drug-Target Kinetics in Drug Discovery. *ACS Chem. Neurosci. 9*, 29−39.

(28) Copeland, R. A. (2016) The drug-target residence time model: a 10-year retrospective. *Nat. Rev. Drug Discovery 15*, 87−95.

(29) Swinney, D. C. (2009) The role of binding kinetics in therapeutically useful drug action. *Curr. Opin. Drug Discovery Dev. 12*, 31−39.

(30) Morrison, J. F., and Walsh, C. T. (2006) The behavior and significance of slow-binding enzyme inhibitors. *Adv. Enzymol. Relat. Areas Mol. Biol. 61*, 201−301.

(31) Morrison, J. F. (1982) The Slow-Binding and Slow, Tight-Binding Inhibition of Enzyme-Catalyzed Reactions. *Trends Biochem. Sci. 7*, 102−105.

(32) Johnson, K. A., Simpson, Z. B., and Blom, T. (2009) Global kinetic explorer: a new computer program for dynamic simulation and fitting of kinetic data. *Anal. Biochem. 387*, 20−9.

(33) Yu, W., Neckles, C., Chang, A., Bommineni, G. R., Spagnuolo, L., Zhang, Z., Liu, N., Lai, C., Truglio, J., and Tonge, P. J. (2015) A [(32)P]NAD(+)-based method to identify and quantitate long residence time enoyl-acyl carrier protein reductase inhibitors. *Anal. Biochem. 474*, 40−9.

(34) Kharlamova, A. D., Lushchekina, S. V., Petrov, K. A., Kots, E. D., Nachon, F., Villard-Wandhammer, M., Zueva, I. V., Krejci, E., Reznik, V. S., Zobov, V. V., Nikolsky, E. E., and Masson, P. (2016) Slow-binding inhibition of acetylcholinesterase by an alkylammonium derivative of 6-methyluracil: mechanism and possible advantages for myasthenia gravis treatment. *Biochem. J. 473*, 1225−36.

(35) Ticha, A., Stanchev, S., Vinothkumar, K. R., Mikles, D. C., Pachl, P., Began, J., Skerle, J., Svehlova, K., Nguyen, M. T. N., Verhelst, S. H. L., Johnson, D. C., Bachovchin, D. A., Lepsik, M., Majer, P., and Strisovsky, K. (2017) General and Modular Strategy for Designing Potent, Selective, and Pharmacologically Compliant Inhibitors of Rhomboid Proteases. *Cell Chem. Biol. 24*, 1523−1536.e4.

(36) Van Aller, G. S., Nandigama, R., Petit, C. M., DeWolf, W. E., Jr., Quinn, C. J., Aubart, K. M., Zalacain, M., Christensen, S. B., Copeland, R. A., and Lai, Z. (2005) Mechanism of time-dependent inhibition of polypeptide deformylase by actinonin. *Biochemistry 44*, 253−260.

(37) Hansen, R., Peters, U., Babbar, A., Chen, Y., Feng, J., Janes, M. R., Li, L. S., Ren, P., Liu, Y., and Zarrinkar, P. P. (2018) The reactivity-driven biochemical mechanism of covalent KRAS(G12C) inhibitors. *Nat. Struct. Mol. Biol. 25*, 454.

(38) Hulme, E. C., and Trevethick, M. A. (2010) Ligand binding assays at equilibrium: validation and interpretation. *Br. J. Pharmacol. 161*, 1219−37.

DOI: 10.1021/acsinfecdis.9b00012
ACS Infect. Dis. 2019, 5, 796−808

(39) Bigott-Hennkens, H. M., Dannoon, S., Lewis, M. R., and Jurisson, S. S. (2008) In vitro receptor binding assays: general methods and considerations. *Q. J. Nucl. Med. Mol. Imaging 52*, 245−253.
(40) Guo, D., Heitman, L. H., and IJzerman, A. P. (2017) Kinetic Aspects of the Interaction between Ligand and G Protein-Coupled Receptor: The Case of the Adenosine Receptors. *Chem. Rev. 117*, 38−66.
(41) Gunther, J. R., Du, Y., Rhoden, E., Lewis, I., Revennaugh, B., Moore, T. W., Kim, S. H., Dingledine, R., Fu, H., and Katzenellenbogen, J. A. (2009) A set of time-resolved fluorescence resonance energy transfer assays for the discovery of inhibitors of estrogen receptor-coactivator binding. *J. Biomol. Screening 14*, 181−193.
(42) Vasta, J. D., Corona, C. R., Wilkinson, J., Zimprich, C. A., Hartnett, J. R., Ingold, M. R., Zimmerman, K., Machleidt, T., Kirkland, T. A., Huwiler, K. G., Ohana, R. F., Slater, M., Otto, P., Cong, M., Wells, C. I., Berger, B.-T., Hanke, T., Glas, C., Ding, K., Drewry, D. H., Huber, K. V. M., Willson, T. M., Knapp, S., Müller, S., Meisenheimer, P. L., Fan, F., Wood, K. V., and Robers, M. B. (2018) Quantitative, Wide-Spectrum Kinase Profiling in Live Cells for Assessing the Effect of Cellular ATP on Target Engagement. *Cell Chem. Biol. 25*, 206.
(43) Andruska, N., Mao, C., Cherian, M., Zhang, C., and Shapiro, D. J. (2012) Evaluation of a luciferase-based reporter assay as a screen for inhibitors of estrogen-ERalpha-induced proliferation of breast cancer cells. *J. Biomol. Screening 17*, 921−32.
(44) Renaud, J. P., Chung, C. W., Danielson, U. H., Egner, U., Hennig, M., Hubbard, R. E., and Nar, H. (2016) Biophysics in drug discovery: impact, challenges and opportunities. *Nat. Rev. Drug Discovery 15*, 679−98.
(45) Day, E. S., Cote, S. M., and Whitty, A. (2012) Binding efficiency of protein-protein complexes. *Biochemistry 51*, 9124−36.
(46) Rich, R. L., and Myszka, D. G. (2010) Grading the commercial optical biosensor literature-Class of 2008: 'The Mighty Binders'. *J. Mol. Recognit. 23*, 1−64.
(47) Schuck, P. (1997) Use of surface plasmon resonance to probe the equilibrium and dynamic aspects of interactions between biological macromolecules. *Annu. Rev. Biophys. Biomol. Struct. 26*, 541−566.
(48) Giannetti, A. M., Koch, B. D., and Browner, M. F. (2008) Surface plasmon resonance based assay for the detection and characterization of promiscuous inhibitors. *J. Med. Chem. 51*, 574−80.
(49) Leavitt, S., and Freire, E. (2001) Direct measurement of protein binding energetics by isothermal titration calorimetry. *Curr. Opin. Struct. Biol. 11*, 560−6.
(50) Gruner, S., Neeb, M., Barandun, L. J., Sielaff, F., Hohn, C., Kojima, S., Steinmetzer, T., Diederich, F., and Klebe, G. (2014) Impact of protein and ligand impurities on ITC-derived protein-ligand thermodynamics. *Biochim. Biophys. Acta, Gen. Subj. 1840*, 2843−50.
(51) Velazquez-Campoy, A., and Freire, E. (2006) Isothermal titration calorimetry to determine association constants for high-affinity ligands. *Nat. Protoc. 1*, 186−91.
(52) Di Trani, J. M., De Cesco, S., O'Leary, R., Plescia, J., do Nascimento, C. J., Moitessier, N., and Mittermaier, A. K. (2018) Rapid measurement of inhibitor binding kinetics by isothermal titration calorimetry. *Nat. Commun. 9*, 893.
(53) Hansen, L. D., Transtrum, M. K., Quinn, C., and Demarse, N. (2016) Enzyme-catalyzed and binding reaction kinetics determined by titration calorimetry. *Biochim. Biophys. Acta, Gen. Subj. 1860*, 957−966.
(54) Bockman, M. R., Engelhart, C. A., Dawadi, S., Larson, P., Tiwari, D., Ferguson, D. M., Schnappinger, D., and Aldrich, C. C. (2018) Avoiding Antibiotic Inactivation in Mycobacterium tuberculosis by Rv3406 through Strategic Nucleoside Modification. *ACS Infect. Dis. 4*, 1102−1113.
(55) O'Shannessy, D. J., Brigham-Burke, M., Soneson, K. K., Hensley, P., and Brooks, I. (1993) Determination of Rate and Equilibrium Binding Constants for Macromolecular Interactions Using Surface Plasmon Resonance: Use of Nonlinear Least Squares Analysis Methods. *Anal. Biochem. 212*, 457−468.
(56) Damian, L. (2013) in *Protein-Ligand Interactions. Methods in Molecular Biology (Methods and Protocols)* (Williams, M., and Daviter, T., Eds.), Vol. *1008*, Humana Press, Totowa, NJ.
(57) Li, H. J., Lai, C. T., Pan, P., Yu, W., Liu, N., Bommineni, G. R., Garcia-Diaz, M., Simmerling, C., and Tonge, P. J. (2014) A structural and energetic model for the slow-onset inhibition of the Mycobacterium tuberculosis enoyl-ACP reductase InhA. *ACS Chem. Biol. 9*, 986−93.
(58) Feng, B. Y., and Shoichet, B. K. (2006) A detergent-based assay for the detection of promiscuous inhibitors. *Nat. Protoc. 1*, 550−3.

DOI: 10.1021/acsinfecdis.9b00012
ACS Infect. Dis. 2019, 5, 796−808